1   **Challenges and opportunities in population monitoring of cheetahs**

2

3   Daniel W. Linden[1][*][℮], David S. Green[2][§][*][℮], Elena V. Chelysheva[3], Salim Mandela[3], and Stephanie

4   M. Dloniak[2]

5   [1] NOAA National Marine Fisheries Service, Greater Atlantic Regional Fisheries Office,

6   Gloucester, MA 01930, USA

7   [2] Department of Integrative Biology, Michigan State University, East Lansing, MI, 45524, USA

8   [3] Mara-Meru Cheetah Project, Nairobi, Kenya

9

10   [*] Corresponding author: daniel.linden@noaa.gov

11   [§] Current address: Institute for Natural Resources, Oregon State University, Corvallis, OR,

12   97331, USA

13   [℮] These authors contributed equally.

14

15   **Keywords:** *Acinonyx jubatus*, cheetah, Masai Mara National Reserve, Mara-Serengeti

16   ecosystem, non-invasive sampling, population monitoring, spatial-capture recapture

Abstract

Population monitoring is key to wildlife conservation and management but is challenging at the spatial and temporal extents necessary for understanding changes. Non-invasive survey methods and spatial capture-recapture (SCR) models have revolutionized wildlife monitoring by providing the means to more easily acquire data at large scales and the framework to generate spatially-explicit predictions, respectively. Despite the opportunities for improved monitoring, challenges can remain in the study design and model fitting phases of an SCR approach. Here, we used a search-encounter design with multi-session SCR models to collect spatially-indexed photographs and estimate the changes in density of cheetahs between 2005 and 2013–2016 in the Masai Mara National Reserve (MMNR) in southwestern Kenya. Our SCR models of cheetah encounters suggested little change in cheetah density from 2005 to 2013–2016, though there was some evidence that density fluctuated annually in the MMNR. The sampling period length (5 vs. 10 months) and timing (early, late, full year) over which spatial encounters were included in the modeling did not substantially alter inferences about density when sample sizes were adequate (>20 spatially distinct encounters). We estimated an average cheetah density of ~1.2 cheetahs/100 km^2, consistent with the impression that the MMNR provides important habitat for cheetahs in Africa. During most years and seasonal periods, the spatial distribution of vegetation greenness (a proxy for ungulate habitat quality) accounted for important variation in encounter rates. The search-encounter design used here could be applied to other regions for the purposes of cheetah monitoring. While snap-shot estimates of population size across time are useful for wildlife monitoring, open population models could identify the mechanisms behind changes and further facilitate better conservation and management decision making.

Introduction

Population monitoring is key to wildlife conservation and management but is challenging at the spatial and temporal extents necessary for understanding changes (Ellis et al. 2014). Monitoring over space and time requires a feasible scheme and persistence in both dedication and resources to obtain adequate information. Low replication in either dimension reduces the capacity to explain observed patterns or test hypotheses about perturbation, limiting the value of the monitoring data for informing conservation and management decisions (Yoccoz et al. 2001). The monitoring challenge has been particularly acute for wide-ranging, cryptic species that occur at low densities, such as carnivores. These life history features have historically made data collection and analysis difficult and reduced the opportunities for robust inference about population dynamics at relevant spatial and temporal scales (Karanth et al. 2006).

Non-invasive survey methods (Long et al. 2008) and spatial capture-recapture (SCR) models (Borchers and Efford 2008, Royle et al. 2014) have revolutionized wildlife population monitoring by providing the means to more easily acquire data at large scales and the framework to generate spatially-explicit predictions, respectively. In an SCR model, the locations of individual encounters (e.g., photographs, genetic material) are used to determine centers of activity for each observed individual, providing spatial information on the number of total individuals in the population and the probabilities of encountering them across the landscape. By formally linking the distributions of individuals and their movement ecology in a hierarchical framework, SCR models jointly estimate the ecological and observational processes that generate the spatial encounter data collected by large-scale monitoring designs, enabling robust inferences that are critical for conservation (Royle et al. 2018). These models have proven useful for estimating the density of wide-ranging carnivores, particularly in applications to large felids including tigers *Panthera tigris* (Royle et al. 2009), jaguars *Panthera onca* (Sollmann et al. 2011), leopards *Panthera pardus* (Gray and Prum 2012) and cougars *Puma concolor* (Russell et al. 2012). Recently, the approach was illustrated using search-encounter surveys with African lions *Panthera leo* (Elliot and Gopalaswamy 2017) and cheetahs *Acinonyx jubatus* (Broekhuis and Gopalaswamy 2016). These applications have highlighted the potential of SCR as a monitoring tool, though rarely have studies spanned long enough timeframes to allow for examining temporal changes in population size or density at large scales (e.g., Chandler and Clark 2014).

70 Despite the opportunities for improved monitoring, challenges can remain in the study

71 design and model fitting phases of a spatial capture-recapture approach. Sampling efforts may

72 not yield enough unique spatial locations per individual to enable model fitting (Becker et al.

73 2017), unless some type of auxiliary data is integrated (e.g., telemetry; Sollmann et al. 2013).

74 Longer survey durations can be used to acquire more captures or encounters, at the expense of

75 potentially violating assumptions regarding population closure (i.e., no births, deaths,

76 immigrants/emigrants during sampling). The timing and duration of surveys will dictate the

77 scope of the population being assessed, dependent on which individuals are available for

78 sampling (e.g., residents vs. dispersers) and can meet assumptions of the observation process.

79 Resource selection at one or more spatial scales can affect model inferences if not properly

80 incorporated, particularly if it results in unmodeled heterogeneity in the encounter process

81 (Royle et al. 2013, Linden et al. 2018). And small sample sizes, even when large enough to

82 enable model fitting, may yet afford little power for accommodating relevant variation in one or

83 more parameters which can reduce accuracy and precision of the resulting estimates (Sollmann

84 et al. 2013). Most of these design and modeling considerations are important for any animal

85 sampling and population estimation approach, and we note that explicitly modeling the sampling

86 process does not necessarily obviate critical assumptions regarding how data were collected and

87 what the data represent. For these reasons and others, it is prudent that researchers design robust

88 monitoring schemes, use multiple lines of evidence, and temper any conclusions from

89 monitoring data when making inferences that will guide conservation and management of large

90 carnivore populations.

91 Here, we used a search-encounter design with SCR models (sensu Royle et al. 2011) to

92 collect spatially-indexed photographs and estimate the changes in density of cheetahs between

93 2005 and 2013–2016 in the Masai Mara National Reserve (MMNR) in southwestern Kenya.

94 Cheetahs are currently listed globally as "vulnerable" with a decreasing total population (Durant

95 et al. 2015, Durant et al. 2017) and while much of the current cheetah range exists outside of

96 protected areas the populations within represent important strongholds for cheetah conservation

97 (Durant et al. 2017). Few long-term studies have empirically estimated how cheetah populations

98 are faring over time (Chauvenet et al. 2011, Durant et al. 2011), or have illustrated how changing

99 landscapes around protected areas may be influencing wildlife within reserve boundaries.

100 Carnivore populations in the MMNR have historically been high compared to other areas in sub-

4

101 Saharan Africa (Craft et al. 2015), and the Mara-Serengeti ecosystem is considered a stronghold

102 for large carnivores in East Africa (Ogutu and Dublin 2002, Riggio et al. 2013). Yet,

103 populations of wild herbivores in the MMNR have been declining over time (Ottichilo et al.

104 2000, Ogutu et al. 2009, Ogutu et al. 2011), livestock often graze within reserve boundaries and

105 anthropogenic disturbance has altered the behaviors and population numbers of other large

106 carnivores (Boydston et al. 2003, Kolowski and Holekamp 2009, Green et al. 2018a), and

107 rangelands around the MMNR are rapidly shifting into a matrix of urbanization and agriculture

108 (Lamprey and Reid 2004, Løvschal et al. 2017).

109   Broekhuis and Gopalaswamy (2016) recently provided a 2014 population estimate for

110 cheetahs within the greater Mara using a similar survey and SCR modeling approach. We fit

111 more extensive data from a multi-year survey effort (2005, 2013–2016) conducted during a

112 longer sampling window (10 months) with sample sizes that afforded additional model

113 complexity. In particular, we incorporated a resource selection function relating the probability

114 of encounter to annual variance in green vegetation (i.e., Normalized Difference Vegetation

115 Index [NDVI]) as an approximation to habitat quality for ungulate prey (Pettorelli et al. 2005,

116 Bro-Jorgensen et al. 2008). We hypothesized that cheetahs would be encountered more

117 frequently in areas with high variation where vegetation changed drastically across the year in

118 response to moisture (e.g., short grass), compared to low variance regions with relatively

119 constant conditions (e.g., riparian forest or bare ground). We also compared inferences between

120 5-month (both an early and late season) and 10-month sampling periods to explore tradeoffs in

121 the acquisition of encounters while trying to meet population closure assumptions.

122   Our earlier initial modeling efforts suggested a >50% decline in cheetah density between

123 2005 and 2013 (Green et al. 2014), but the population estimate by Broekhuis and Gopalaswamy

124 (2016) challenged that conclusion. Additional years of monitoring and subsequent modeling

125 indicate that the Mara cheetah population may exhibit annual fluctuations due to movement

126 between the MMNR, adjacent conservancies, and the Serengeti National Park, highlighting the

127 importance of conservation and management efforts in those areas surrounding the reserve.

128

Materials and Methods

Study area and data collection

Our study took place in the 1510 km^2 Masai Mara National Reserve in southwestern Kenya (Figure 1). The MMNR is predominantly comprised of open grassland interspersed with riparian areas, supporting a high density and diversity of resident herbivores, which are also joined seasonally by migrant populations of wildebeest *Connochaetes taurinus*, zebra *Equus quagga*, and Thomson's gazelle *Eudorcas thomsonii* from the Serengeti National Park to the southwest and the Loita plains to the northeast (Bell 1971, Stelfox et al. 1986, Sinclair and Norton-Griffiths 1995). The MMNR is bounded by the border with Tanzania and the Serengeti National Park to the south, and is surrounded in all other directions by community conservancies, pastoralist communities, small towns, and agricultural lands (Figure 1). There are no fences or barriers encompassing the MMNR, and wildlife regularly move beyond its political borders.

We systematically searched for cheetahs in the MMNR from January to October in 2005 and each year during 2013–2016 by dividing the MMNR into 6 sampling blocks roughly equal in size (Figure S1). Searches occurred between 0500 and 1900 h, during which time observers (1 or 2) drove throughout one block looking for cheetahs in a single vehicle, periodically stopping and scanning the surrounding landscape with binoculars (Caro 1994). Main roads were followed when convenient but considerable time was spent off-road to cover all accessible areas of each block; survey effort was calculated as the number of hours spent searching a block on a given date. When a cheetah was sighted, we drove within 50 m of an individual or group of individuals and photographed both sides of each animal and recorded geographic coordinates, sex and age class. We identified each individual using the distinct pelage and tail ring patterns (Caro and Durant 1991) and limited our modeling to adults.

We acquired spatial raster data from the Famine Early Warning System Network hosted by the USGS/EROS Data Center (https://earlywarning.usgs.gov/fews/). The data included 250 m resolution grids with 10-day NDVI values observed across each year (36 for a given year) for a region spanning most of East Africa. We calculated the standard deviation in NDVI value within a given year to approximate the seasonal variation within a given grid cell. Notable features that are apparent in every year include the vegetation along the Mara and Talek Rivers (Figure S2).

6

160   *Spatial capture-recapture model*

161   Similar to previous applications of spatial capture-recapture using unstructured search-

162   encounter designs (Russell et al. 2012, Broekhuis and Gopalaswamy 2016), we divided our study

163   area (the MMNR) into a grid with a sufficiently low resolution (2-km × 2-km cells) to create

164   spatial encounter histories for individual cheetahs. We defined the number of encounters y_{ij} for

165   individual i in grid cell j as a Poisson-distributed random variable:

166 $$y_{ij} \sim \text{Poisson}(\lambda_{ij} g_{ij})$$

167   Here, λ_{ij} is the mean encounter rate for an individual having its activity center (s_i) within a given

168   grid cell, and g_{ij} is a detection function describing how encounter rate decreases as the distance

169   (d_{ij}) increases between the location of an individual's activity center and the coordinates of grid

170   cell j. We chose a Gaussian encounter probability model such that $g_{ij} = \exp(-d_{ij}^2/2\sigma^2)$, where σ is

171   a scale parameter representing the standard deviation of a bivariate normal distribution used to

172   approximate space usage (Royle et al. 2014). While sex is often used as a factor for describing

173   variation in σ (Sollmann et al. 2011, Broekhuis and Gopalaswamy 2016), our early model fitting

174   did not indicate a difference between females and males or among years; σ remained constant in

175   our final model specification.

176   The mean encounter rate λ_{ij} was modeled as a function of several variables specific to an

177   individual and grid cell. We considered differences among years to account for potential factors

178   related to observers and the space-use of individual cheetahs in a given year. We also considered

179   two grid cell covariates for λ_{ij}: 1) the annual variance in NDVI for each year (standardized within

180   the year to have mean = 0 and unit variance); and 2) the log-transformed fraction of hours spent

181   searching a grid cell, given its location within 1 of the 6 search blocks. We included quadratic

182   functions for NDVI that were year-specific to accommodate resource selection by cheetahs in

183   response to spatial-temporal differences in vegetation within the Mara across years. The effect

184   of search effort was constrained similar to a Poisson offset, though we estimated a regression

185   coefficient instead of assuming it was 1. As such, we modeled the log-linear encounter rate (λ_{ij})

186   as:

187              $$\log(\lambda_{ij}) = \alpha_0 + \alpha_{1,\text{yr}} + \alpha_{2,\text{yr}} \, \text{NDVI}_{\text{yr}[i],j} + \alpha_{3,\text{yr}} \, \text{NDVI}_{\text{yr}[i],j}^2 + \alpha_4 \, \text{EFFORT}_{\text{yr}[i],j}$$

188   Here, α_0 is the baseline encounter rate on the log scale for an individual captured in 2005; $\alpha_{1,\text{yr}}$ is

189   a vector of year-specific coefficients for differences in encounter rates of individuals observed in

7

190   later years (yr[i] = 2013, 2014, 2015, or 2016); $\alpha_{2,yr}$ and $\alpha_{3,yr}$ are vectors of year-specific

191   coefficients for the linear and quadratic effects, respectively, of the variance in NDVI for each

192   grid cell in each year; and α_4 is a coefficient describing the relationship between encounter rate

193   and search effort in a given grid cell and year. We considered encounters separated by ≥5 days

194   to represent independent events with regards to individual movement and encounter probability

195   and, therefore, thinned 18–35% of the total encounters in a given year to help meet model

196   assumptions. Adult male cheetahs regularly form coalitions with other males (Caro and Collins

197   1987) and we observed them doing so in the MMNR (~60% of male sightings involved

198   coalitions). Despite this, we treated each sighting as an independent observation given that

199   coalitions were sometimes observed to exhibit fission-fusion dynamics and that the

200   independence assumption for activity centers has been shown to be robust to departures (Reich

201   and Gardner 2014).

202   We modeled the distribution of latent activity centers using an inhomogeneous point

203   process (Borchers and Efford 2008) to estimate variation in cheetah density over the years. We

204   expanded the 2-km resolution grid of the MMNR to include a 20-km buffer (Figure S1), which

205   was large enough to ensure a negligible encounter probability at the edges (Royle et al. 2014);

206   we also excluded the northwest escarpment, which was likely to have restricted cheetah

207   movement (Broekhuis and Gopalaswamy 2016). The total state space, S, of the point process

208   therefore included 1,381 discrete grid cells for a total area of 5,524 km^2. The intensity of the

209   point process (i.e., the expected density) within a grid cell j in a given year was a log-linear

210   function:

211   $$\log(\mathrm{E}(D_{j,yr})) = \beta_0 + \beta_{1,yr}$$

212   Here, β_0 is the log-scale expected cheetah density in 2005, while $\beta_{1,yr}$ is a vector of year-specific

213   regression coefficients that estimate differences in expected density in later years (yr = 2013,

214   2014, 2015, or 2016). Conditional on the expected density for the year in which an individual

215   was encountered (yr$_i$), the probability of an individual's activity center being located within a

216   given grid cell was defined as:

217   $$\Pr(s_i = j \mid \boldsymbol{\beta}, yr_i) = \frac{\mathrm{E}(D_{j,yr})}{\sum\limits_{j} \mathrm{E}(D_{j,yr})}$$

218   The marginal likelihood of the observations for each individual are then computed by integrating

219   over all possible grid cells.

220

221   *Model fitting and sample period comparison*

222   We fit the model using the multi-session sex-structured SCR framework in the R package

223   `oSCR` (Sutherland et al. 2016) which maximizes the Poisson-integrated likelihood (Borchers and

224   Efford 2008) and provides maximum likelihood estimates of model parameters. In addition to

225   the parameters previously described, `oSCR` allows for estimating a sex ratio (ψ). Without

226   specification of sex-specific parameters in the other SCR model components, estimates of ψ are

227   derived entirely from the observed sex ratios of encountered individuals during each session

228   (here, session = year).

229   We compared several sampling periods (early 5 months, full 10 months, late 5 months) to

230   examine how differences in the observed data and parameter estimates affected population

231   inferences. The early period spanned Jan–May and corresponded to a mostly hot and dry season

232   that turns into long and heavy rains by May. The late period spanned Jun–Oct and corresponded

233   to the cool season that follows the heavy rain season, during which widespread green vegetation

234   supports a massive ungulate migration (Bell 1971, Sinclair and Norton-Griffiths 1995). This late

235   period was similar to the 3-month sampling design (August–October) used by Broekhuis and

236   Gopalaswamy (2016). The full 10-month sampling period spanned most of the year (Jan–Oct)

237   and, while facilitating more observations and larger sample sizes of individuals and spatial

238   encounters, was likely to violate the assumption of population closure to a greater degree than

239   the 5-month periods. Aside from differences in the density estimates across time we were

240   particularly interested in how other model parameters might change with variation in the number

241   and type of spatial encounters, including the estimated NDVI relationships with encounter rate,

242   sex ratios, and individual movement scale.

243

244   **Results**

245   Monitoring efforts resulted in >7000 hours spent searching for and recording observations of

246   cheetahs in the MMNR during 2005 and 2013–2016. The average number of hours searched

247   each year was 1443 (range: 1086–1694) for the 10-month sampling period, which split into 623

248   (range: 513–790) for the early 5-month period and 820 (range: 573–989) for the late 5-month

9

249 period (Table 1). Compared to either 5-month period, the increased sampling effort for the full

250 10 months always resulted in greater numbers (within a given year) of unique individuals

251 encountered (median across years: full = 32, early = 20, late = 23), total encounter events (full =

252 101, early = 40, late = 60), and spatially distinct encounters (full = 58, early = 18, late = 28).

253 The observed sex ratios were variable depending on the year and sampling period, though on a

254 whole the median ratio was 1:1. We plotted the unique individuals encountered each year

255 according to the midpoint ordinal date of their encounters, indicating the sampling period(s) in

256 which they were observed (Figure 2). The patterns indicated similar ratios of females to males

257 observed during all sampling period definitions.

258 The spatial capture-recapture models indicated similar patterns in density variation over

259 time (Table 2–3; Figure 3), though fluctuations were mostly small relative to the uncertainty.

260 The density estimates from 2005 had very large confidence intervals for the 5-month sampling

261 periods due to small sample sizes. The full period density estimate (with 95% CI) for 2005 was

262 1.62 (1.02–2.57) cheetahs/100 km^2. During 2013–2016, mean estimated density ranged from

263 0.60 (0.34–1.10) cheetahs/100 km^2 in 2013 to 1.63 (0.97–2.73) cheetahs/100 km^2 in 2014, and

264 estimates matched closely across sampling periods within a given year. Precision of the density

265 estimates was better for the 10-month sampling period, particularly with regards to the

266 coefficients of variation (Table 3). Regardless of the sampling period, density estimates with a

267 CV <0.30 could be achieved with >20 spatially distinct encounters (Figure 4).

268 The relationships between encounter rate and NDVI variance were variable across years

269 and across sampling periods within a year (Table 2; Figure 5). For most years and sampling

270 periods, the maximum encounter rates occurred at mid to high values of relative NDVI variance.

271 The early period in 2016 was the primary exception, suggesting higher encounter rates for

272 cheetahs in low variance areas during Jan–May. The hours spent searching a grid cell (given the

273 survey block within which it was located) had a strong positive relationship with encounter rate,

274 and average encounter rates were higher in later years (2013–2016) compared to 2005. The scale

275 parameter of the half-normal distance function was much smaller for the early 5-month period (σ

276 = 4.9 km [4.4–5.4 km]) compared to the late 5-month period (σ = 8.1 km [7.2–9.2 km]) and the

277 full 10-month period (σ = 7.0 km [6.4–7.5 km]).

10

278   The sex ratios were estimated to be largely even across all years and sampling periods as

279 none of the logit-scale estimates were significantly different from 0 (Table 2), suggesting that the

280 probability of an individual being a male did not vary considerably from 0.50.

281

Discussion

283   Effective wildlife population monitoring spans enough time and space to detect change or

284 variation that may require further investigation or be targeted for management action. In

285 addition to adequate spatial and temporal extents, the sampling intensity needs to produce

286 enough observations to ensure reasonable precision from statistical models designed to estimate

287 population parameters. Our spatial capture-recapture models of cheetah encounters suggested

288 little change in cheetah density from 2005 to 2013–2016 in the Masai Mara National Reserve,

289 though there was some evidence that density fluctuated annually in recent years. The sampling

290 period length (5 vs. 10 months) and timing (early, late, full year) over which spatial encounters

291 were included in the modeling did not substantially alter inferences about density when sample

292 sizes were adequate (e.g., $\geq$20 spatially distinct encounters). This suggests some flexibility in the

293 design of search-encounter surveys for monitoring cheetahs over large landscapes.

294   We estimated an average cheetah density of ~1.2 cheetahs/100 km^2, consistent with the

295 impression that the MMNR provides important habitat for cheetahs in Africa. Cheetah density

296 varies extensively throughout the current species range, from 0.02 cheetahs/100 km^2 in areas of

297 low productivity (Belbachir et al. 2015) to >2 cheetahs/100 km^2 in the highly productive

298 Serengeti (Durant et al. 2011, Durant et al. 2017). Broekhuis and Gopalaswamy (2016) used a

299 similar search encounter design with SCR modeling and estimated a mean cheetah density of

300 ~1.3 cheetahs/100 km^2 in the MMNR and surrounding conservancies in 2014, which is

301 consistent with our 2014 estimate from the late period (1.37 cheetahs/100 km^2). Our additional

302 years of monitoring indicated that density in some years may be nearly half that which was

303 estimated in 2014.

304   Long-term studies of cheetah population trends in the Mara-Serengeti ecosystem have

305 indicated a relatively stable density in recent years (Chauvenet et al. 2011, Durant et al. 2011). If

306 the density fluctuation we estimated during 2013–2016 represents a real ecological phenomenon,

307 as opposed to sampling variability, then our comparison with 2005 is difficult to interpret, given

308 that this single year could have represented either ebb or flow for the cheetah population.

11

309   Therefore, it is actually unclear whether cheetah density has declined in the MMNR during the

310   past 10+ years. This uncertainty highlights the value of long-term monitoring programs, but also

311   of monitoring designs that can estimate population size with useful precision. Our population

312   modeling was limited to adult cheetahs and many individuals were encountered during only a

313   portion of the year (Figure 2), therefore, population fluctuation in the MMNR is likely due to

314   variable movement between the reserve and surrounding areas (e.g., Serengeti National Park).

315   The magnitude of individual movements in cheetahs could make annual density an erratic

316   statistic for an area the size of the MMNR (1510 km^2), especially in the presence of non-resident,

317   "floater" males (Caro 1994). Density estimation from SCR modeling is generally robust to

318   transient individuals, though such movement dynamics could be explicitly modeled (Royle et al.

319   2016).

320   Based on the estimate of σ from the distance function, the mean 95% space use or home

321   range area ranged from ~450 to ~1,200 km^2 in the MMNR. Cheetah home ranges can be similar

322   in size for males and females and overlap in areas where prey are non-migratory (Broomhall et

323   al. 2003). In contrast, where ungulate prey are migratory, home ranges are comparatively larger

324   with males forming small territories and females exhibiting roving behaviors (Caro 1994).

325   Although there is a seasonal influx of migrant herbivores into the MMNR each year (Bell 1971,

326   Stelfox et al. 1986, Sinclair and Norton-Griffiths 1995), resident herbivores are also present year-

327   round in relatively high numbers. Thus, movements by cheetahs in the MMNR may be better

328   predicted by interspecific competition with other large carnivores (Broekhuis et al. 2013) or the

329   direct and indirect effects of people, rather than habitat suitability or prey populations. We

330   caution any interpretation of the 95% space use approximation given the circular assumption of

331   the bivariate normal distribution for σ (Royle et al. 2014). In addition, cheetah space use has

332   been shown to be highly concentrated within a small portion of the home range (~14% of the

333   total area), even for individuals that otherwise occupy large areas (Marker et al. 2008).

334   Several differences between our study and that of Broekhuis and Gopalaswamy (2016;

335   hereafter, B&G) warrant discussion, given the similarity in our approaches to collecting and

336   modeling spatial encounters of cheetahs in the Mara. First, B&G modeled the daily encounter

337   probability over 90 days of sampling, while we summed our encounters over the relevant

338   sampling period (5 or 10 months) and treated the counts as a Poisson random variable; given the

339   low rates of encounter, these choices should have had a negligible influence (Royle et al. 2014).

340   Second, our definitions of effort differed and B&G's approach was preferable: using GPS tracks

341   to define exactly which areas were searched. We did not have GPS track records for 2005 and

342   instead attempted to systematically search pre-defined sections (i.e., blocks) of the MMNR for

343   various lengths of time; such a definition of effort is approximate at best, though blocks were

344   searched thoroughly when visited. Third, we observed a fairly even sex ratio of cheetahs that

345   remained constant over the 5 years of surveys and is consistent with previous research in the

346   Mara-Serengeti (Kelly et al. 1998). The extremely skewed ratio observed by B&G (F:M = 5:1)

347   was potentially an artefact of a low sample size and short survey duration (3 months), though it

348   should also be noted that most of their survey effort was in the conservancies to the north of the

349   MMNR. Finally, B&G estimated a difference in the scale parameter (σ) between females and

350   males; early data exploration here did not support such differences in our study, both given the

351   observed maximum distances moved and preliminary estimates of σ from models with sex-

352   specific parameters. Despite these differences, the close similarity in cheetah density estimates

353   provides empirical support to the robustness of SCR modeling (Royle et al. 2014).

354   Improvements to the design of our search-encounter survey could make the effort more

355   efficient and useful in other parts of the species range. We thinned almost 1/3 of our observed

356   cheetah encounters before fitting the SCR models because of uneven effort across space and

357   time. Ideally, areas would be searched with regular periodicity to ensure that inferences

358   regarding individual movement matched in temporal scale at all spatial locations. This is

359   typically the case for other common methods of collecting spatial encounters (e.g., camera

360   trapping), where traps are operated on regular intervals (Royle et al. 2014). The problem of

361   sampling regularity would be most acute for transient individuals; for example, 5 consecutive

362   days of effort in a given location could yield a very different collection of encounters than 5 days

363   spread across several months. Uneven spatial sampling makes the interpretation of posterior

364   density surfaces from SCR models especially problematic and prone to artefacts (Efford 2018a),

365   relegating the identification of "hot spots" (e.g., Broekhuis and Gopalaswamy 2016) to random

366   error. Finally, the ability to traverse the landscape and get close enough to individuals for high

367   quality photographs could limit the application of this survey to certain regions (e.g., protected

368   areas). While long-range camera lenses may provide expanded opportunities for monitoring, it

369   could still be difficult to clearly photograph both sides of every individual at great distances,

370   ultimately increasing identification uncertainty (Augustine et al. 2018).

13

371   Other aspects of cheetah population ecology could be modeled with different or more

372   complex analytical approaches to the individual encounter data we generated with the surveys.

373   Our primary objective was a comparison between 2005 and 2013–2016, so we focused on

374   understanding how best to estimate density within a given year (or seasonal period), while

375   accommodating the sparse data from 2005. We hypothesized that individual space use and, thus,

376   encounter probability would vary by habitat attributes and used NDVI variance as a proxy for

377   ungulate habitat quality (Pettorelli et al. 2005, Bro-Jorgensen et al. 2008); in most years and

378   seasonal periods, the spatial distribution of NDVI variance accounted for important variation in

379   encounter rates. An open population model (Kendall et al. 1997) would allow for estimating

380   survival and temporary emigration and potentially enable more comprehensive inferences than

381   "snap-shot" density estimates (Harmsen et al. 2017). While open-population SCR models

382   provide the opportunity to integrate spatial explicitness into estimation and prediction (e.g.,

383   Green et al. 2018b), the Bayesian frameworks typically used for fitting such models are

384   notoriously slow and computationally demanding for complex spatiotemporal inferences. New

385   approaches using maximum likelihood and hidden Markov models could provide promising

386   alternatives (Glennie et al. 2017, Efford 2018b). Snap-shot estimates of population size across

387   time are useful for wildlife monitoring, but understanding the mechanisms behind population

388   changes can facilitate better conservation and management decision making (Harmsen et al.

389   2017).

390

398

Authorship

400   DWL, DSG, SMD, and EC designed the study. SMD, EC, and SM conducted the

401   fieldwork, and DWL completed the modeling. All authors contributed to the manuscript writing.

Data accessibility

Data will be archived with Dryad Digital Repository.

References

Augustine, B. C., J. A. Royle, M. J. Kelly, C. B. Satter, R. S. Alonso, E. E. Boydston, and K. R. Crooks. 2018. Spatial capture-recapture with partial identity: An application to camera traps. Annals of Applied Statistics 12:67-95.

Becker, M. S., S. M. Durant, F. G. R. Watson, M. Parker, D. Gottelli, J. M'soka, E. Droge, M. Nyirenda, P. Schuette, S. Dunkley, and R. Brummer. 2017. Using dogs to find cats: detection dogs as a survey method for wide-ranging cheetah. Journal of Zoology 302:184-192.

Belbachir, F., N. Pettorelli, T. Wacher, A. Belbachir-Bazi, and S. M. Durant. 2015. Monitoring rarity: the critically endangered Saharan cheetah as a flagship species for a threatened ecosystem. Plos One 10:e0115136.

Bell, R. H. 1971. A grazing ecosystem in the Serengeti. Scientific American 225:86-93.

Borchers, D. L. and M. G. Efford. 2008. Spatially explicit maximum likelihood methods for capture-recapture studies. Biometrics 64:377-385.

Boydston, E. E., K. M. Kapheim, H. E. Watts, M. Szykman, and K. E. Holekamp. 2003. Altered behaviour in spotted hyenas associated with increased human activity. Pages 207-219 *in* Animal Conservation forum. Cambridge University Press.

Bro-Jorgensen, J., M. E. Brown, and N. Pettorelli. 2008. Using the satellite-derived normalized difference vegetation index (NDVI) to explain ranging patterns in a lek-breeding antelope: the importance of scale. Oecologia 158:177-182.

Broekhuis, F., G. Cozzi, M. Valeix, J. W. McNutt, and D. W. Macdonald. 2013. Risk avoidance in sympatric large carnivores: reactive or predictive? Journal of Animal Ecology 82:1098-1105.

Broekhuis, F. and A. M. Gopalaswamy. 2016. Counting Cats: Spatially Explicit Population Estimates of Cheetah (Acinonyx jubatus) Using Unstructured Sampling Data. Plos One 11:e0153875.

Broomhall, L., M. Mills, and J. Du Toit. 2003. Home range and habitat use by cheetahs (Acinonyx jubatus) in the Kruger National Park. Journal of Zoology 261:119-128.

15

Caro, T. 1994. Cheetahs of the Serengeti Plains: group living in an asocial species. University of Chicago Press.

Caro, T. and D. Collins. 1987. Male cheetah social organization and territoriality. Ethology 74:52-64.

Caro, T. and S. Durant. 1991. Use of quantitative analyses of pelage characteristics to reveal family resemblances in genetically monomorphic cheetahs. Journal of Heredity 82:8-14.

Chandler, R. B. and J. D. Clark. 2014. Spatially explicit integrated population models. Methods in Ecology and Evolution 5:1351-1360.

Chauvenet, A. L., S. M. Durant, R. Hilborn, and N. Pettorelli. 2011. Unintended consequences of conservation actions: managing disease in complex ecosystems. Plos One 6:e28671.

Craft, M. E., K. Hampson, J. O. Ogutu, and S. M. Durant. 2015. Carnivore communities in the greater Serengeti ecosystem. Pages 419-450 *in* A. R. E. Sinclair, K. L. Metzger, S. A. R. Mduma, and J. M. Fryxell, editors. Serengeti IV: sustaining biodiversity in a coupled human-natural system. The University of Chicago Press, Chicago, USA.

Durant, S., N. Mitchell, A. Ipavec, and R. Groom. 2015. Acinonyx jubatus. The IUCN Red List of Threatened Species 2015. e. T219A50649567.

Durant, S. M., M. E. Craft, R. Hilborn, S. Bashir, J. Hando, and L. Thomas. 2011. Long-term trends in carnivore abundance using distance sampling in Serengeti National Park, Tanzania. Journal of Applied Ecology 48:1490-1500.

Durant, S. M., N. Mitchell, R. Groom, N. Pettorelli, A. Ipavec, A. P. Jacobson, R. Woodroffe, M. Böhm, L. T. B. Hunter, M. S. Becker, F. Broekhuis, S. Bashir, L. Andresen, O. Aschenborn, M. Beddiaf, F. Belbachir, A. Belbachir-Bazi, A. Berbash, I. Brandao de Matos Machado, C. Breitenmoser, M. Chege, D. Cilliers, H. Davies-Mostert, A. J. Dickman, F. Ezekiel, M. S. Farhadinia, P. Funston, P. Henschel, J. Horgan, H. H. de Iongh, H. Jowkar, R. Klein, P. A. Lindsey, L. Marker, K. Marnewick, J. Melzheimer, J. Merkle, J. M'soka, M. Msuha, H. O'Neill, M. Parker, G. Purchase, S. Sahailou, Y. Saidu, A. Samna, A. Schmidt-Küntzel, E. Selebatso, E. A. Sogbohossou, A. Soultan, E. Stone, E. van der Meer, R. van Vuuren, M. Wykstra, and K. Young-Overton. 2017. The global decline of cheetah *Acinonyx jubatus* and what it means for conservation. Proceedings of the National Academy of Sciences 114:528-533.

16

463   Efford, M. G. 2018a. Density surfaces in secr 3.1. http://www.otago.ac.nz/density/pdfs/secr-
464   densitysurfaces.pdf Last Accessed 23 Feb 2018.

465   Efford, M. G. 2018b. openCR: Open Population Capture-Recapture. R package version 1.3.2.
466   https://cran.r-project.org/package=openCR.

467   Elliot, N. B. and A. M. Gopalaswamy. 2017. Toward accurate and precise estimates of lion
468   density. Conservation Biology 31:934-943.

469   Ellis, M. M., J. S. Ivan, and M. K. Schwartz. 2014. Spatially explicit power analyses for
470   occupancy-based monitoring of wolverine in the U.S. Rocky Mountains. Conservation
471   Biology 28:52-62.

472   Glennie, R., D. L. Borchers, M. Murchie, B. J. Harmsen, and R. J. Foster. 2017. Open population
473   maximum likelihood spatial capture-recapture. Submitted to Biometrics.
474   http://hdl.handle.net/10023/11758.

475   Gray, T. N. E. and S. Prum. 2012. Leopard density in post-conflict landscape, Cambodia:
476   Evidence from spatially explicit capture-recapture. Journal of Wildlife Management
477   76:163-169.

478   Green, D. S., L. Johnson-Ulrich, H. E. Couraud, and K. E. Holekamp. 2018a. Anthropogenic
479   disturbance induces opposing population trends in spotted hyenas and African lions.
480   Biodiversity and Conservation 27:871-889.

481   Green, D. S., D. W. Linden, E. V. Chelysheva, and S. M. Dloniak. 2014. Estimating changes in
482   cheetah density and distribution in the Mara-Serengeti ecosystem with spatial capture-
483   recapture (SCR). The Wildlife Society 21st Annual Conference, Pittsburgh, PA. DOI:
484   10.13140/RG.2.2.34678.86086.

485   Green, D. S., S. M. Matthews, R. C. Swiers, R. L. Callas, J. Scott Yaeger, S. L. Farber, M. K.
486   Schwartz, and R. A. Powell. 2018b. Dynamic occupancy modelling reveals a hierarchy of
487   competition among fishers, grey foxes and ringtails. Journal of Animal Ecology 87:813-
488   824.

489   Harmsen, B. J., R. J. Foster, E. Sanchez, C. E. Gutierrez-González, S. C. Silver, L. E. T. Ostro,
490   M. J. Kelly, E. Kay, and H. Quigley. 2017. Long term monitoring of jaguars in the
491   Cockscomb Basin Wildlife Sanctuary, Belize; Implications for camera trap studies of
492   carnivores. Plos One 12:e0179505.

17

493   Karanth, K. U., J. D. Nichols, N. S. Kumar, and J. E. Hines. 2006. Assessing tiger population

494   dynamics using photographic capture–recapture sampling. Ecology 87:2925-2937.

495   Kelly, M. J., M. K. Laurenson, C. D. FitzGibbon, D. A. Collins, S. M. Durant, G. W. Frame, B.

496   C. Bertram, and T. Caro. 1998. Demography of the Serengeti cheetah (Acinonyx jubatus)

497   population: the first 25 years. Journal of Zoology 244:473-488.

498   Kendall, W. L., J. D. Nichols, and J. E. Hines. 1997. Estimating temporary emigration using

499   capture–recapture data with Pollock's robust design. Ecology 78:563-578.

500   Kolowski, J. and K. Holekamp. 2009. Ecological and anthropogenic influences on space use by

501   spotted hyaenas. Journal of Zoology 277:23-36.

502   Lamprey, R. H. and R. S. Reid. 2004. Expansion of human settlement in Kenya's Maasai Mara:

503   what future for pastoralism and wildlife? Journal of Biogeography 31:997-1032.

504   Linden, D. W., A. P. K. Sirén, and P. J. Pekins. 2018. Integrating telemetry data into spatial

505   capture–recapture modifies inferences on multi-scale resource selection. Ecosphere

506   9:e02203.

507   Long, R. A., P. MacKay, J. Ray, and W. Zielinski. 2008. Noninvasive survey methods for

508   carnivores. Island Press, Washington, DC, USA.

509   Løvschal, M., P. K. Bøcher, J. Pilgaard, I. Amoke, A. Odingo, A. Thuo, and J.-C. Svenning.

510   2017. Fencing bodes a rapid collapse of the unique Greater Mara ecosystem. Scientific

511   Reports 7:41450.

512   Marker, L., A. Dickman, M. G. Mills, R. Jeo, and D. W. Macdonald. 2008. Spatial ecology of

513   cheetahs on north-central Namibian farmlands. Journal of Zoology 274:226-238.

514   Ogutu, J. and H. Dublin. 2002. Demography of lions in relation to prey and habitat in the Maasai

515   Mara National Reserve, Kenya. African Journal of Ecology 40:120-129.

516   Ogutu, J. O., N. Owen-Smith, H. P. Piepho, and M. Y. Said. 2011. Continuing wildlife

517   population declines and range contraction in the Mara region of Kenya during 1977-

518   2009. Journal of Zoology 285:99-109.

519   Ogutu, J. O., H. P. Piepho, H. Dublin, N. Bhola, and R. S. Reid. 2009. Dynamics of Mara–

520   Serengeti ungulates in relation to land use changes. Journal of Zoology 278:1-14.

521   Ottichilo, W. K., J. De Leeuw, A. K. Skidmore, H. H. Prins, and M. Y. Said. 2000. Population

522   trends of large non-migratory wild herbivores and livestock in the Masai Mara

523   ecosystem, Kenya, between 1977 and 1997. African Journal of Ecology 38:202-216.

18

Pettorelli, N., J. O. Vik, A. Mysterud, J. M. Gaillard, C. J. Tucker, and N. C. Stenseth. 2005. Using the satellite-derived NDVI to assess ecological responses to environmental change. Trends in Ecology & Evolution 20:503-510.

Reich, B. J. and B. Gardner. 2014. A spatial capture-recapture model for territorial species. Environmetrics 25:630-637.

Riggio, J., A. Jacobson, L. Dollar, H. Bauer, M. Becker, A. Dickman, P. Funston, R. Groom, P. Henschel, and H. de Iongh. 2013. The size of savannah Africa: a lion's (Panthera leo) view. Biodiversity and Conservation 22:17-35.

Royle, J. A., R. B. Chandler, R. Sollmann, and B. Gardner. 2014. Spatial capture-recapture. Academic Press, Waltham, MA, USA.

Royle, J. A., R. B. Chandler, C. C. Sun, and A. K. Fuller. 2013. Integrating resource selection information with spatial capture-recapture. Methods in Ecology and Evolution 4:520-530.

Royle, J. A., A. K. Fuller, and C. Sutherland. 2016. Spatial capture-recapture models allowing Markovian transience or dispersal. Population Ecology 58:53-62.

Royle, J. A., A. K. Fuller, and C. Sutherland. 2018. Unifying population and landscape ecology with spatial capture–recapture. Ecography 41:444-456.

Royle, J. A., K. U. Karanth, A. M. Gopalaswamy, and N. S. Kumar. 2009. Bayesian inference in camera trapping studies for a class of spatial capture-recapture models. Ecology 90:3233-3244.

Royle, J. A., M. Kéry, and J. Guelat. 2011. Spatial capture-recapture models for search-encounter data. Methods in Ecology and Evolution 2:602-611.

Russell, R. E., J. A. Royle, R. Desimone, M. K. Schwartz, V. L. Edwards, K. P. Pilgrim, and K. S. McKelvey. 2012. Estimating abundance of mountain lions from unstructured spatial sampling. Journal of Wildlife Management 76:1551-1561.

Sinclair, A. R. E. and M. Norton-Griffiths. 1995. Serengeti: dynamics of an ecosystem. University of Chicago Press.

Sollmann, R., M. M. Furtado, B. Gardner, H. Hofer, A. T. A. Jacomo, N. M. Torres, and L. Silveira. 2011. Improving density estimates for elusive carnivores: Accounting for sex-specific detection and movements using spatial capture-recapture models for jaguars in central Brazil. Biological Conservation 144:1017-1024.

19

554   Sollmann, R., B. Gardner, R. B. Chandler, D. B. Shindle, D. P. Onorato, J. A. Royle, and A. F.

555   O'Connell. 2013. Using multiple data sources provides density estimates for endangered

556   Florida panther. Journal of Applied Ecology 50:961-968.

557   Stelfox, J. G., D. G. Peden, H. Epp, R. J. Hudson, S. W. Mbugua, J. L. Agatsiva, and C. L.

558   Amuyunzu. 1986. Herbivore dynamics in southern Narok, Kenya. The Journal of

559   Wildlife Management 50:339-347.

560   Sutherland, C., J. A. Royle, and D. W. Linden. 2016. oSCR: Multi-Session Sex-Structured

561   Spatial Capture-Recapture Models. R package version 0.30.1.

562   https://github.com/jaroyle/oSCR.

563   Yoccoz, N. G., J. D. Nichols, and T. Boulinier. 2001. Monitoring of biological diversity in space

564   and time. Trends in Ecology & Evolution 16:446-453.

565

Tables

Table 1. Summary of monitoring effort and adult cheetah encounters in the Masai Mara National Reserve during 2005 and 2013–2016. Results from the 3 sampling periods (early 5 months [Jan–May], full 10 months [Jan–Oct], and late 5 months [Jun–Oct]) include the hours spent searching, the number of unique individuals encountered (n) and broken down by sex (F/M), and the number of encounter events (y). Spatially distinct encounters occur across >1 grid cell and by definition involve recapture of an individual. For example, in 2005 there were 23 individuals encountered during the early 5-month period but only 8 (4 female; 4 male) were encountered in >1 grid cell.

Months	Year	Hrs	Total encounters			Spatially distinct encounters		
			n	(F/M)	y>0	n	(F/M)	y>1
5 (Jan–May)	2005	513	23	(12/11)	34	8	(4/4)	11
	2013	790	12	(6/6)	34	6	(3/3)	18
	2014	530	20	(10/10)	40	13	(8/5)	19
	2015	705	24	(11/13)	68	12	(6/6)	39
	2016	578	20	(12/8)	41	7	(6/1)	16
10 (Jan–Oct)	2005	1086	26	(14/12)	47	14	(7/7)	21
	2013	1535	20	(10/10)	73	13	(9/4)	46
	2014	1465	34	(14/20)	112	26	(12/14)	73
	2015	1694	32	(13/19)	142	19	(10/9)	92
	2016	1438	32	(17/15)	101	22	(12/10)	58
5 (Jun–Oct)	2005	573	11	(7/4)	13	2	(0/2)	2
	2013	745	15	(10/5)	39	8	(6/2)	22
	2014	935	30	(13/17)	72	17	(5/12)	39
	2015	989	23	(10/13)	74	12	(7/5)	45
	2016	860	27	(14/13)	60	14	(9/5)	28

21

Table 2. Parameter estimates from the spatial capture-recapture models of adult cheetah encounters in 2005 and 2013–2016 in the Masai Mara National Reserve, fit to data from the early period (Jan–May), full period (Jan–Oct), and late period (Jun–Oct). Estimates are on the scale of the appropriate link function, either log (α, β) or logit (ψ).

Process	θ	Effect	early (Jan–May)		full (Jan–Oct)		late (Jun–Oct)	
			Estimate	SE	Estimate	SE	Estimate	SE
Encounter	α_0	Intercept	−3.915	0.362	−4.277	0.301	−5.345	0.756
	$\alpha_{1,2013}$	Year	1.261	0.459	0.784	0.319	1.732	0.790
	$\alpha_{1,2014}$		0.730	0.454	0.945	0.302	1.648	0.778
	$\alpha_{1,2015}$		1.089	0.408	0.998	0.303	1.660	0.782
	$\alpha_{1,2016}$		1.373	0.445	0.850	0.308	1.075	0.786
	$\alpha_{2,2005}$	NDVI×Year	1.284	0.485	0.366	0.232	−0.560	0.386
	$\alpha_{2,2013}$		1.167	0.393	0.709	0.252	0.621	0.344
	$\alpha_{2,2014}$		−1.684	0.491	−0.157	0.155	0.254	0.196
	$\alpha_{2,2015}$		0.961	0.335	0.775	0.219	0.580	0.297
	$\alpha_{2,2016}$		−0.413	0.247	0.143	0.148	0.823	0.298
	$\alpha_{3,2005}$	NDVI^2×Year	−0.920	0.397	−0.369	0.225	−0.245	0.382
	$\alpha_{3,2013}$		−0.675	0.392	−0.731	0.284	−0.879	0.442
	$\alpha_{3,2014}$		−1.569	0.458	−0.609	0.174	−0.636	0.230
	$\alpha_{3,2015}$		−0.377	0.228	−0.257	0.145	−0.130	0.187
	$\alpha_{3,2016}$		−0.408	0.219	−0.127	0.125	−0.236	0.211
	α_4	Effort	0.874	0.151	0.703	0.130	0.691	0.149
	$\log(\sigma)$	Dist. scale	1.583	0.055	1.940	0.039	2.094	0.065
Density	β_0	Intercept	−2.243	0.291	−2.732	0.236	−2.760	0.682
	$\beta_{1,2013}$	Year	−1.474	0.418	−0.668	0.328	−0.791	0.735
	$\beta_{1,2014}$		−0.491	0.389	−0.146	0.294	−0.147	0.709
	$\beta_{1,2015}$		−0.867	0.358	−0.415	0.295	−0.659	0.714
	$\beta_{1,2016}$		−0.904	0.379	−0.316	0.297	−0.246	0.714
Sex ratio	ψ_{2005}	Pr(M)×Year	−0.087	0.417	−0.154	0.393	−0.560	0.627
	ψ_{2013}		0.000	0.577	0.000	0.447	−0.693	0.548
	ψ_{2014}		0.000	0.447	0.357	0.348	0.268	0.368
	ψ_{2015}		0.167	0.410	0.379	0.360	0.262	0.421
	ψ_{2016}		−0.405	0.456	−0.125	0.354	−0.074	0.385

579   Table 3. Mean estimates (with standard errors and coefficients of variation) of cheetah density

580   (#/100 km^2) from the spatial capture-recapture models of adult cheetah encounters in 2005 and

581   2013–2016 in the Masai Mara National Reserve, fit to data from the early period (Jan–May), full

582   period (Jan–Oct), and late period (Jun–Oct).

| Year	early (Jan–May)			full (Jan–Oct)			late (Jun–Oct)		
	Mean	SE	CV	Mean	SE	CV	Mean	SE	CV
2005	2.65	0.77	0.29	1.63	0.38	0.24	1.58	1.08	0.68
2013	0.61	0.18	0.30	0.83	0.19	0.23	0.72	0.20	0.28
2014	1.62	0.43	0.26	1.41	0.25	0.18	1.37	0.28	0.20
2015	1.12	0.24	0.21	1.07	0.19	0.18	0.82	0.18	0.22
2016	1.07	0.27	0.25	1.19	0.22	0.18	1.24	0.27	0.22

23

Figures

583 **Figures**

584 Figure 1. The location of cheetah monitoring in the Masai Mara National Reserve (MMNR) in

585 southwestern Kenya (35.125º E, 1.44º S). Other conservation areas (shaded) surround the

586 MMNR, including the Serengeti National Park in Tanzania to the south. Map data ©

587 OpenStreetMap contributors, CC BY-SA.

588   Figure 2. The midpoint ordinal date of encounter for each individual cheetah and the sampling

589   periods in which they were encountered in the Masai Mara during 2005 and 2013–2016. Note,

590   any individuals with encounters that spanned the full period (10 months) were included in the

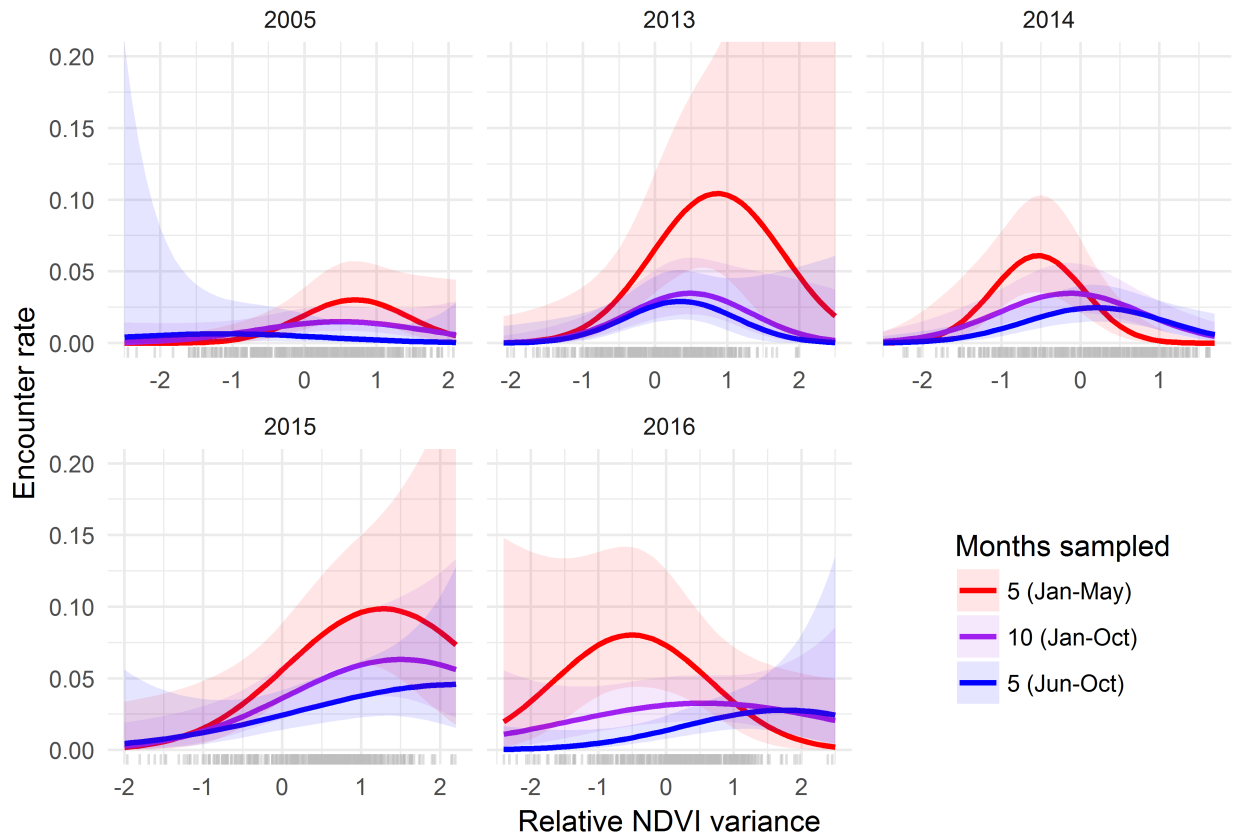591   spatial capture-recapture models for all 3 periods.
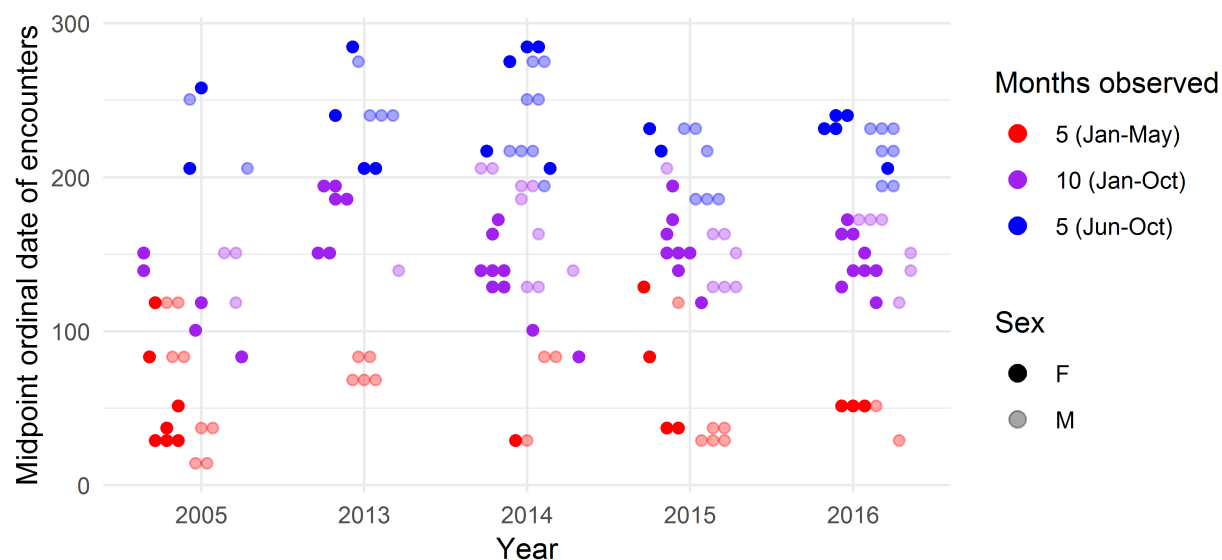
592   Figure 3. Mean estimates (with 95% CI) of cheetah density (#/100 km^2) in the Masai Mara

593   National Reserve in 2005 and 2013–2016 from spatial capture-recapture models fit using 5

594   months (early and late periods) and 10 months of surveys.
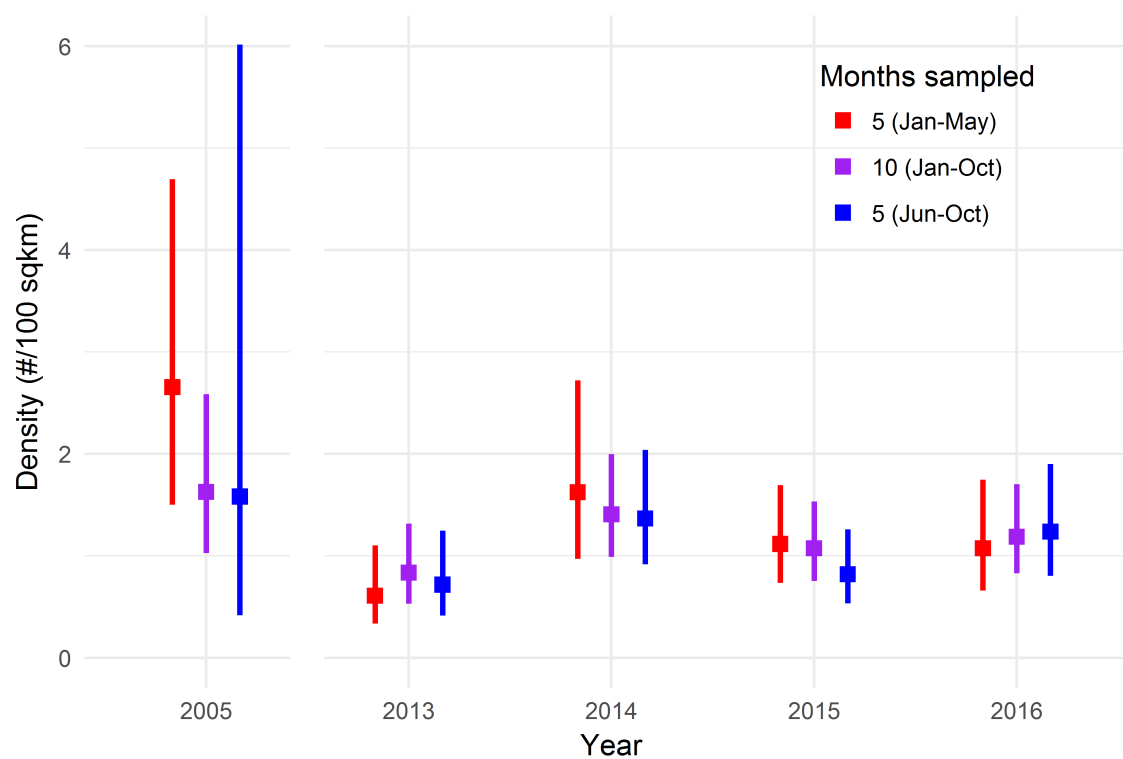
595   Figure 4. Relationship between number of spatially distinct encounters and coefficients of

596   variation (CVs) for density estimates from the spatial capture-recapture models. Spatially

597   distinct encounters occur across >1 grid cell and by definition involve recapture of an individual.


27
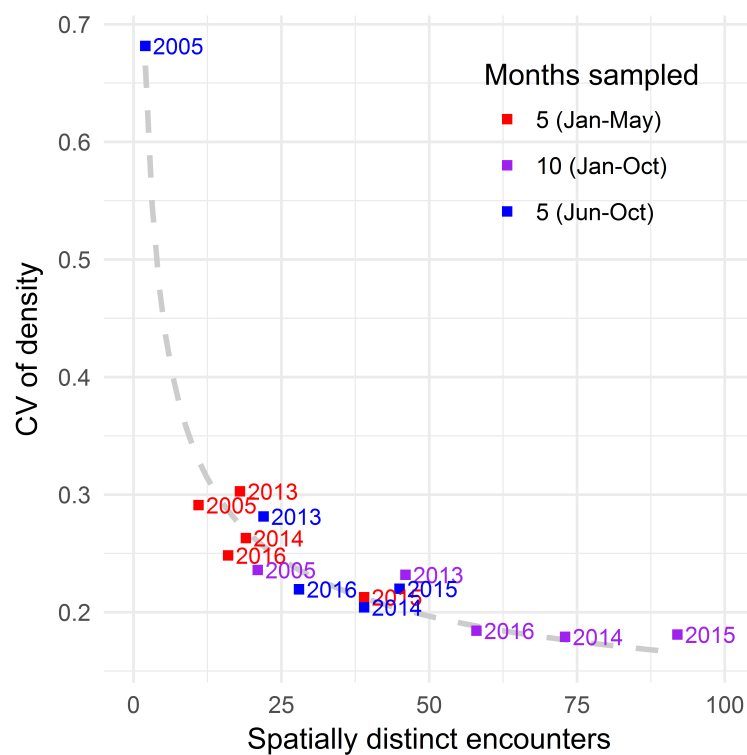
598   Figure 5. Predicted relationships (with 95% CI) between NDVI variance and cheetah encounter

599   rate during 2005 and 2013–2016 from spatial capture-recapture models using 5 months (early

600   and late periods) and 10 months of surveys. Values for NDVI variance were standardized to

601   have mean 0 and unit variance within each year. Ticks at bottom indicate observed values at

602   pixel locations within the MMNR.

603 **Supplements**

604 Figure S1. Grid cells illustrating state space used in the spatial capture-recapture models, with

605 delineations of blocks according to survey effort. Light gray cells occurred in areas not searched

606 but included as a buffer for population estimation.
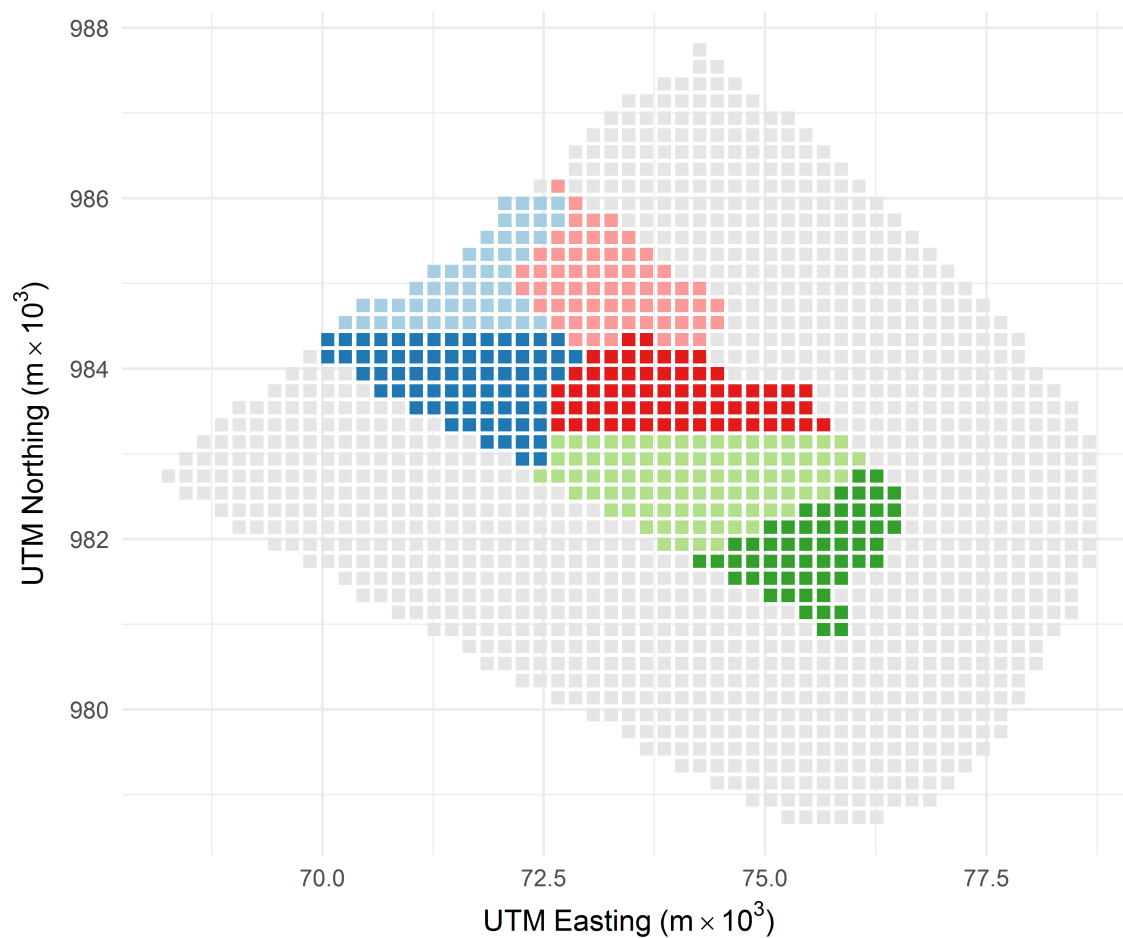
607   Figure S2. Spatial distributions of Normalized Vegetation Difference Index (NDVI) values in

608   each year that served as covariates for encounter probability in the spatial capture-recapture

609   models. Values represent the variance (standard deviation) in NDVI across the 36 satellite

610   images (10-day intervals at 250 m resolution) for a given year. NDVI values were mean

611   aggregated to the 2-km grid cells and standardized within each year to have mean of zero and

612   unit variance.   Satellite images acquired from the Famine Early Warning System Network

613   hosted by the USGS/EROS Data Center (https://earlywarning.usgs.gov/fews/).